ChemPubSoc Europe

DOI: 10.1002/chem.201800849

CHEMISTRY A European Journal Full Paper

Surface Chemistry |Hot Paper|

BN-Patterning of Metallic Substrates through Metal Coordination of Decoupled Borazines

Martin Schwarz[+],[a] Manuela Garnica[+],[a] Francesco Fasano[+],[b] Nicola Demitri,[c] Davide Bonifazi,*[b] and Willi Auwärter*[a]

Abstract: We report on the synthesis of pyridine-terminated borazine derivatives, their molecular self-assembly as well as the electronic properties investigated on silver and copper surfaces by means of scanning tunneling microscopy and X-ray photoelectron spectroscopy. The introduction of pyridine functionalities allows us to achieve distinct supramolecular architectures with control of the interdigitation of the molecules by surface templating. On silver surfaces, the borazine derivatives arrange in a dense-packed hexagonal structure through van der Waals and H-bonding interactions, whereas on Cu(111), the molecules undergo metal coordination. The porosity and coordination symmetry of the reticulated structure depends on the stoichiometric ratio between copper adatoms and the borazine ligands, permitting an unusual three-fold coordinated Cu–pyridyl network. Finally, spectroscopy measurements show that the borazine core is electronically decoupled from the metallic substrate. We thus demonstrate that BNC-containing molecular units can be integrated in stable metal-coordination architectures on surfaces, opening pathways to patterned, BN-doped sheets with specific functionalities, for example, regarding the adsorption of polar guest gases.

Introduction

Borazine derivatives have recently attracted increasing interest as molecular building blocks,[1,2] due to their high potential for applications in the fields of electronics,[3–6] and non-linear optics.[7] In particular hybrid *h*-BNC nanostructures, where carbon-carbon bonds are replaced by isoelectronic and isostructural BN couples are emerging as a new route to functionalize polycyclic aromatic hydrocarbons without a significant structural perturbation of the molecular periphery and of its skeleton.[6,8] The presence of BN bonds imparts strong local dipole moments that can tailor both, the optoelectronic properties and the self-assembly behavior of the molecule.[9,10] For instance, one can conjecture that the polar BN bonds could serve as anchoring point for non-covalent adsorption of polar gases like CO_2 and CO, which can in principle interact with BN bonds through dipolar interactions, thus making BN-doped materials very good candidates for gas adsorption.[11] Together with the possibility of tuning the molecular bandgap into the visible range of the solar spectrum, these structures could emerge as unique photoactive materials triggering photochemical transformations. Given these premises, we conjectured that two-dimensional structures formed through non-covalent interaction on a surface could act as unique model architectures to study the self-assembly and recognition properties of BN-materials at the molecular level through scanning probe microscopy (STM).

In particular, precisely tailored substituents of molecules can be utilized to realize targeted adsorption geometries, as well as to preserve the intrinsic properties of molecules upon adsorption on a metal support.[12] Recently, it has been proposed that a BN core of a molecule can be protected and electronically decoupled from the conductive substrate by di-methyl-phenyl terminal groups through steric hindrance without affecting the possibility of the molecule itself to adsorb and self-assemble.[13] Additionally, the selection of the substituent's termination (e.g.-carbonitrile (CN), -carboxylate, -pyridyl) steers the supramolecular interactions, driving for example the formation of two dimensional metal-organic coordination networks (2D-MOCNs) in the presence of metal adatoms. The formation of such a 2D-MOCN combining borazine and metal adatoms has not been reported to date, although those porous architectures are highly appealing as they can act as templates featuring cavities and molecular units on regular and well-defined sites linked by metallic nodes.[14] Indulging this line of thought, here we describe the synthesis and the self-assembly proper-

[a] M. Schwarz,[+] Dr. M. Garnica,[+] Prof. Dr. W. Auwärter
Department of Physics
Technical University of Munich
85748 Garching (Germany)
E-mail: wau@tum.de

[b] F. Fasano,[+] Prof. Dr. D. Bonifazi
School of Chemistry
Cardiff University
Park Place Main Building, Cardiff CF10 3AT (United Kingdom)
E-mail: bonifazid@cardiff.ac.uk

[c] Dr. N. Demitri
Elettra–Sincrotrone Trieste
S.S. 14 Km 163.5 in Area Science Park, 34149 Basovizza, Trieste (Italy)

[+] These authors contributed equally.

Supporting information and the ORCID identification number(s) for the author(s) of this article can be found under: https://doi.org/10.1002/chem.201800849.

ties of borazine derivatives on Cu(111), Ag(100) and Ag(111) surfaces that, exposing peripheral pyridyl groups, can undergo metal-coordination in the presence of copper adatoms to yield porous patterns. Specifically, STM studies show that the molecules behave differently on the two metals, with those deposited on Ag undergoing self-assembly through weak interactions (van der Waals (vdW) and H-bonding), whereas on Cu the molecules engage in metal-coordination. Using scanning tunneling spectroscopy (STS), we also provide evidence supporting the idea that the borazine core is electronically decoupled from the conductive metal substrate. The architectures on Cu(111) substrates were exposed to CO gas and their chemical properties investigated by XPS. Additionally, we explore the thermal stability of the network on Cu(111) at room temperature, and the effect of post-annealing on both metal substrates by STM.

Synthesis of BNPPy and BNAPy

The pyridine-bearing borazines have been prepared following the BCl_3 condensation protocol (see Supporting Information for synthesis procedure).[4,5] Starting from aniline, which was reacted with BCl_3 under refluxing conditions, a B,B′,B″-trichloro-N,N′,N″-triphenyl borazine intermediate was obtained. Upon subsequent treatment with *tert*-butyldimethylsilyl (TBDMS)-aryllithium (ArLi) **1**, TBDMS protected borazine **2** could be prepared in 78% yield (Scheme 1). Removal of the TBDMS protecting group with TBAF and successive esterification with Tf_2O in pyridine gave tri-triflate borazine **3** in 78% yield. A final Suzuki cross-coupling reaction between molecule **3** and pyridylphenylboronic acid led to the formation of borazine **4** (**BNPPy**) in 87% yield. Crystals suitable for X-ray diffraction analysis were obtained by slow diffusion of pentane in a $CHCl_3$ solution of **1** (Figure 1a). The crystal packing shows hydrophobic contacts between neighbor molecules, with partial π–π stacking involving the aryl arms. The effective packing of **BNPPy** in the solid phase gives rise to a distorted planar arrangement of the molecules, piled up along the crystallographic *c* axis and with partial overlaps of outer pyridine moieties of neighbor molecules (the angle between neighboring borazine ring planes is 53°).

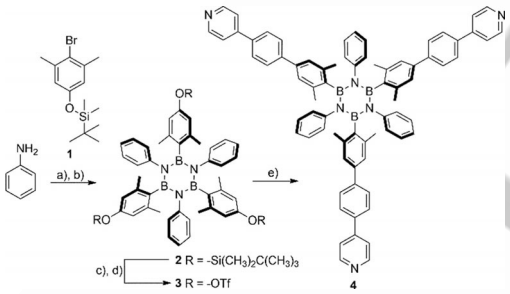

Scheme 1. Synthesis of **BNPPy 4**: a) BCl_3, toluene, reflux, 18 h; b) **1**, *t*BuLi, THF, −84 °C, 2 h, 78%; c) TBAF, THF, 0 °C, 2 h; d) Tf_2O, pyridine, r.t., 16 h, 78%; e) 4-pyridinphenylboronic acid, $[Pd(PPh_3)_4]$, K_2CO_3, dioxane/H_2O (3:1), 105 °C, 18 h, 87%.

Similarly, when a B,B′,B″-trichloro-N,N′,N″-triphenyl borazine intermediate was reacted with trimethylsilyl (TMS)-protected ArLi derivative **5**, TMS-protected borazine derivative **6** could be prepared in 71% yield (Scheme 2). Removal of the silyl protecting group with TBAF yielded phenylacetylenborazine derivative **7**, that could be transformed into borazine **8** (**BNAPy**) by a Sonogashira cross-coupling reaction with 4-iodo-aniline.

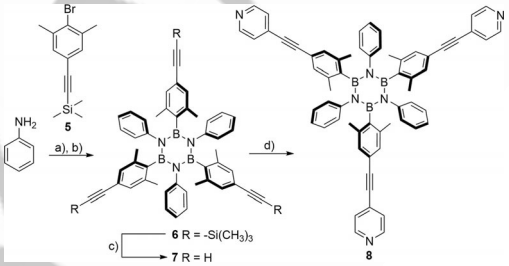

Scheme 2. Synthesis of **BNAPy 8**: a) BCl_3, toluene, reflux, 18 h; b) **5**, *t*BuLi, THF, −84 °C, 16 h, 71%; c) TBAF, THF, 0 °C, 2 h, 94%; d) 4-iodo-pyridine, $[PdCl_2(PPh_3)_2]$, PPh_3, CuI, NEt_3, 75 °C, 17 h, 70%.

Results and Discussion

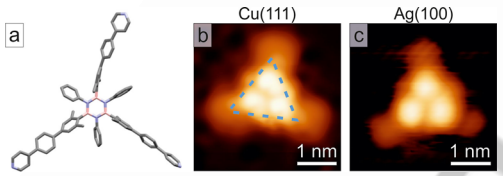

Figure 1. a) Structure of **BNPPy** determined by X-ray diffraction. STM images of an individual **BNPPy** molecule on b) Cu(111) (U_b = 1.9 V, I_t = 170 pA) and c) Ag(100) (U_b = 0.5 V, I_t = 81 pA). The superimposed dashed triangle in b) indicates the orientation of the molecule.

High-resolution STM images of individual **BNPPy** molecules on Cu(111) and Ag(100) show sub-molecular features with a very similar appearance (Figure 1b,c). The central part of the molecule appears as three bright lobes pointing along the axes defined by the pyridyl-terminated substituents, which are imaged dimmer. The molecular contrast does not change for moderate bias voltages of both polarities, suggesting that it reflects the molecular conformation. We simulated STM images for different adsorption geometries using the extended Hückel method (see Supporting Information, Figure S25). The best agreement between experiment and simulation is obtained for a **BNPPy** geometry where the borazine core and the peripheral pyridyl-groups are aligned (nearly) parallel to the surface plane while all phenyl rings are rotated out of this plane. Specifically, the three prominent lobes observed in STM can be reasonably associated with the bulky di-methyl-bearing aryl rings. This assignment is in line with STM observations and complementary molecular dynamics (MD) modeling reported for dimethyl-bearing aryl borazine derivatives on Au(111) and Cu(111).[13] Consistently, we observe a very similar intramolecular contrast featuring three bright protrusions for **BNAPy** on Cu(111) (see Figure 4).

The molecular structure determined by X-ray diffraction on **BNPPY** crystals shows that the expected three-fold symmetry of the molecule can be disturbed due to the flexibility of the

substituents (Figure 1a). Upon adsorption, a similar behavior is observed, as can be seen in Figures 1b,c. The pyridyl-terminated substituents appear bent in the surface plane, resulting in angles enclosed by them deviating from 120°.

The borazine derivative BNPPy on Ag surfaces

Extended, highly ordered molecular islands of **BNPPy** were observed on silver samples with different surface terminations, namely a Ag(100) single crystal and a Ag(111) film (see Figures 2 and 5c, respectively). The molecules, deposited onto the sample held at room temperature, arrange in six-membered rings and form porous honeycomb networks. A similar self-assembly was observed for related molecules on the Au(111) surface.[13] Network domains with sizes of several hundreds of nm and arbitrary orientation with respect to the crystal high-symmetry directions were present on the samples.

A high-resolution close-up view (Figure 2b) reveals that each molecule in the honeycomb structure is surrounded by three neighbors and three pores. The rhombic unit cell (white lines in Figure 2b) has the parameters $a = b = (26.0 \pm 0.5)$ Å and $\theta = (60 \pm 3)°$, which results in a packing density of 0.34 molecules/nm^2. The network is stabilized by intermolecular vdW and H-bonding interactions between the aryl moieties decorating the BN core. The small molecule-molecule distance suggests that the flexible substituents are bent to reduce steric hindrance (see Figure 2c).

Nevertheless, STM-based manipulation experiments indicate weak intermolecular attraction as individual molecules can be removed from the edges of the islands in a controlled fashion without significantly perturbing the self-assembled network (Figure 2d,e). For this purpose, the STM tip is positioned above a rim molecule, which is dragged out to the bare Ag terrace (indicated by the white dashed lines) applying a bias voltage $U_b = 50$ mV and a tunneling current $I_t = 20$ nA. Furthermore, the molecules can be rotated by STM manipulation, changing the orientation of the pyridyl-terminated substituents with respect to the molecular axes (Figure 2f,g). The flexibility of the substituents is clearly revealed in Figure 2f where apparent angles between 90° and almost 180° are observed between adjacent aryl substituents.

In addition to the most abundant arrangement in six-membered rings, a second dense-packed phase (packing density 0.41 molecules/nm^2) embedded in the honeycomb network is occasionally observed (Figure S26). In this phase, **BNPPy** are assembled in rows consisting of pairs of molecules oriented in opposite directions. This pair of molecules constitutes the base unit observed in both structures on the Ag substrates, suggesting that the molecular packing is governed by the same intramolecular interactions and the concentration of molecules on the surface (see Figures 2 and S27). Large coverage deposition promotes the formation of the second phase, which presents a more compact network.

After annealing the sample to 570 K, the hexagonal arrays still occur, including some dislocation lines. Additionally, disordered regions are observed (Figure S27b), where covalent

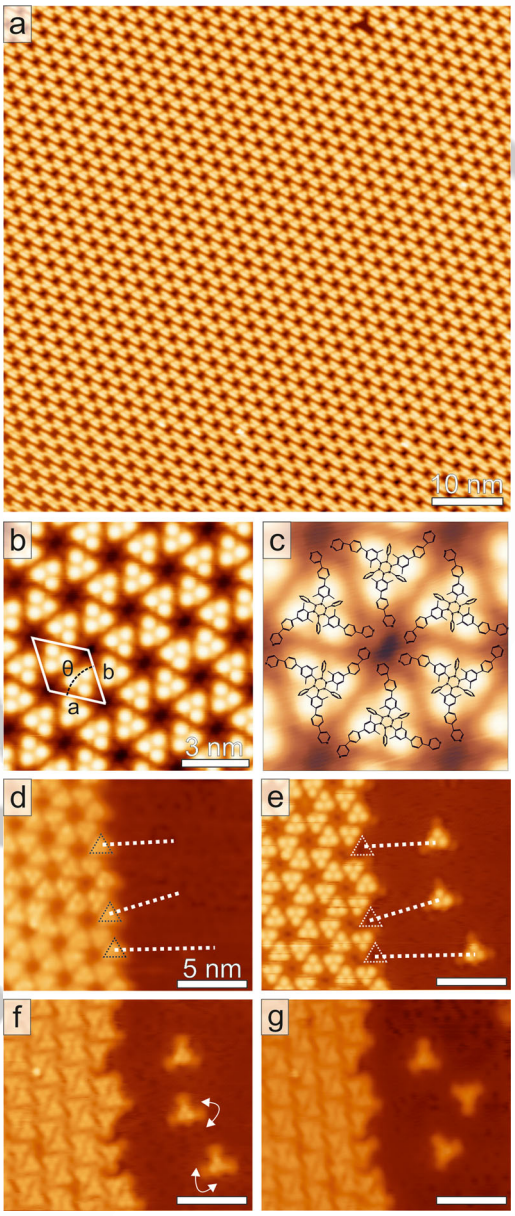

Figure 2. STM images of **BNPPy** on Ag(100). a) Large-scale image of the dense-packed hexagonal network of **BNPPy** molecules. Scan parameters: $U_b = 1.0$ V, $I_t = 64$ pA. b) High-resolution STM image (unit cell highlighted by white rhombus). Scan parameters: $U_b = 0.2$ V, $I_t = 40$ pA. c) STM image overlaid with a tentative structural model of the molecular assembly. d) Individual molecules can be manipulated by STM in a controlled way (dotted white lines represent the tip path). e) Three **BNPPy** molecules were detached from the dense-packed island. (Scan parameters, d,e): $U_b = 0.5$ V, $I_t = 81$ pA). f,g) Additionally, the orientation of the protruding substituents can be changed as indicated by the white arrows in (f). (Scan parameters, f,g): $U_b = 1.7$ V, $I_t = 81$ pA).

structures, formed through thermal activation of C–H bonds, are presumably present.

The borazine derivative BNPPy on Cu(111)

The self-assembly behavior of **BNPPy** molecules on Cu(111) is summarized in Figure 3a. A highly ordered porous 2D network with molecules arranged in interconnected chains (Figure 3d)

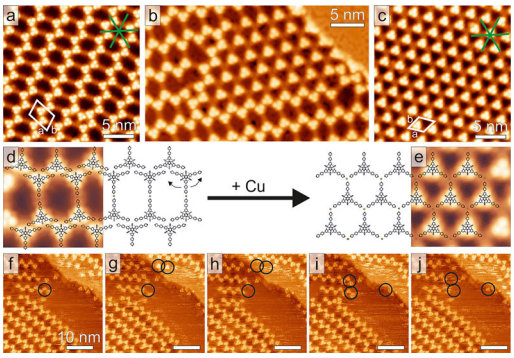

Figure 3. STM images of **BNPPy** on Cu(111). a) Upon room temperature deposition, the **BNPPy** molecules form chains that are interconnected by the protruding substituents coordinated to a Cu adatom. Scan parameters: $U_b = 1.2$ V, $I_t = 100$ pA. b) Deposition of additional Cu atoms with the sample held at 420 K leads to a structural transformation and patches of molecules with all three substituents coordinated to Cu atoms are formed. Scan parameters: $U_b = 1.0$ V, $I_t = 64$ pA. c) With sufficient Cu adatoms available, extended islands with fully three-fold coordinated **BNPPy** molecules are observed. Scan parameters: $U_b = 0.96$ V, $I_t = 40$ pA. d,e) Tentative structural models of the chain-like network and the fully reticulated network superimposed on STM images. f–j) A series of STM images acquired at 300 K shows that the chain-like network is observable at room temperature. Consecutive scans of the same area reveal that individual molecules at the edge of the molecular islands are mobile (highlighted by black circles). Scan parameters: $U_b = 1.0$ V, $I_t = 110$ pA.

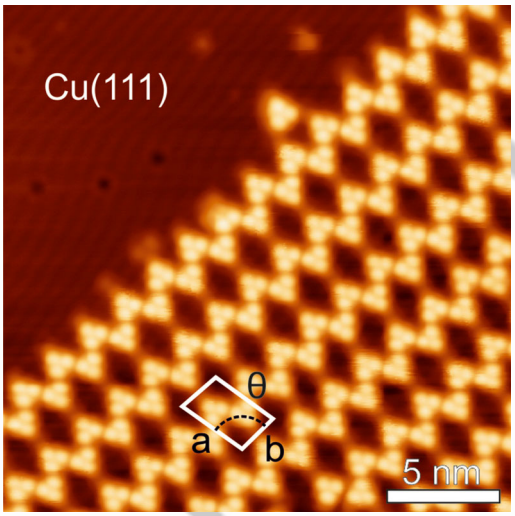

Figure 4. STM image of BNAPy on Cu(111) showing the self-assembly in molecular chains, connected through Cu-coordinated substituents. The trapezoidal unit cell has the parameters a = (32.6 ± 2.6) Å, b = (19.2 ± 2.4) Å, and $\theta = (75 \pm 4)^\circ$. Scan parameters: $U_b = 1.0$ V, $I_t = 100$ pA.

is formed for molecules deposited onto the sample at room temperature. The trapezoidal unit cell of the network has the parameters a = (38.4 ± 2.9) Å, b = (26.5 ± 2.3) Å, and $\theta = (75 \pm 5)^\circ$. The packing density corresponds to 0.20 molecules/nm^2 and the short axis of the unit cell is aligned parallel to one of the $<1\bar{1}0>$ directions of the Cu(111) surface. The growth of the network initiates at step edges. Subsequently, the anisotropic islands expand onto the terraces (Figure S28 a). A similar self-assembled chain-like structure was observed for the borazine derivative **BNAPy** on the same support (see Figure 4). Due to the reduced length of the aryl substituents, the **BNAPy** network presents a smaller trapezoidal unit cell with the parameters a = (32.6 ± 2.6) Å, b = (19.2 ± 2.4) Å, and $\theta = (75 \pm 4)^\circ$.

Along the rows, the molecules are alternately rotated by $(180 \pm 6)^\circ$ and remarkably close-packed. The center-to-center distance ((20.5 ± 0.5) Å for **BNPPy** and (17.9 ± 0.4) Å for **BNAPy**, respectively) suggests that the substituents are slightly bent (Figure 3 d). Adjacent rows are connected via opposing substituents in **BNPPy** and **BNAPy** networks with a center-to-center distance of (32.2 ± 0.6) Å and (27.2 ± 0.5) Å, respectively. This long distance suggests a pyridyl-Cu-pyridyl coordination motif, where the N atoms of the peripheral pyridyl groups are coordinated to a copper atom. Notably, due to the flexibility of the lateral aryl substituents, the molecules are not necessarily connected in a straight line. This results in the formation of a porous network featuring voids of unequal size (Figure S29).[15]

Deposition of additional copper atoms with the sample kept at 420 K gives rise to a structural transformation of the chain-like network: patches of fully Cu-coordinated hexagonal arrays embedded in the former assembly of **BNPPy** on Cu(111) emerge (Figure 3 b). Annealing to this temperature in the absence of extra copper atoms or deposition of the molecules at 420 K does not trigger the formation of this phase. In this new network structure, three **BNPPy** molecules are coordinated with the N atoms of their terminal pyridyl groups to a node that presumably consists of a single Cu atom (see discussion below). As in the previous chain-like assembly, the individual Cu atoms are not resolved in the STM images. Increasing the dose of additional Cu atoms completely transforms the chain-like architecture into a three-fold coordinated, fully reticulated metal-organic network (Figure 3 c,e and Figure S28 b). The trapezoidal unit cell has the parameters a = (25.5 ± 1.7) Å, b = (24.2 ± 1.6) Å with an internal angle $\theta = (60 \pm 2)^\circ$, resulting in a packing density of 0.18 molecules/nm^2. Notably, the nanostructure does not align with the high symmetry directions of the crystal surface.

Further annealing of either network to temperatures higher than 470 K results in a polymeric phase. Contrary to a recent study employing bromine-substituted borazine derivatives aiming for highly regular polymeric nanostructures,[16] only disordered structures were observed. Molecules have presumably lost part of their peripheral substituents and are bond covalently (Figure S27 a). A similar observation was made for the dense-packed structure on Ag, when it was annealed to 570 K (Figure S27 b).

STM measurements performed at 300 K (Figure 3 f–j) reveal that the chain-like **BNPPy** network—comprehensively characterized at 5 K (Figure 3 a)—prevails at room temperature. However, consecutive scans suggest that borazine modules at the edge of molecular islands are mobile, while the bulk of the self-assembled architecture remains mostly unperturbed. Likely, this is a consequence of the weak molecule-substrate interaction combined with the high mobility of Cu adatoms at room temperature that, enabling diffusion of the molecules, allow the dynamic formation and rupture of coordination bonds at the periphery of the self-assembled islands.

Finally, we have carried out XPS measurements on the chain-like network on Cu(111) in order to investigate the ability of the BNPPy molecule to adsorb CO through its central borazine core—thus exploring the potential binding of polar guest gases alluded to in the introduction. XP core-level spectra of a sub-monolayer of BNPPy on Cu(111) before dosing CO are shown in Figure S30. The C 1s core level is observed at a binding energy $E_b = 284.8$ eV. The N 1s core level is found at a binding energy $E_b = 399.2$ eV. Due to its low cross-section, the B 1s core-level could not be resolved for sub-monolayer coverage. In BNPPy multilayers on Cu(111), the C 1s and N 1s core levels (Figure S31) reveal a slight upshift by 0.4 and 0.2 eV, respectively. This is attributed to a suppressed polarization screening by the metallic substrate in case of the multilayer.

After a CO dosage of 60 L at room temperature and a dose of 6 L at $\approx$100 K, no noticeable changes in either core level have been observed in XPS for sub-monolayer coverage. Also in STM measurements no structural changes were detected after an in situ dose of 10 L of CO at temperatures below 15 K. Therefore, we infer that the CO is not adsorbed on the self-assembled network. Presumably, this is caused by the presence of the sterically-hindering methyl substituents that, shielding the B_3N_3 core, impede the formation of favorable dipolar interactions between the BN bonds and CO gas molecules.

Spectroscopic characterization of BNPPy

Scanning tunneling spectroscopy (STS) data of BNPPy on a Cu(111) single crystal and a Ag(111) film are summarized in Figure 5. In the case of Cu(111), the spectra taken in the pore of the chain-like assembly (Figure 5b, blue spectrum) show a pronounced feature at ≈ -400 mV, which is attributed to the increase of the local density of states due to the surface state of Cu(111). This feature is still detected in the spectra taken at the center (red spectrum) and at the bright lobe (yellow spectrum) of the molecule as indicated in Figure 5a. In analogy to reports on other physisorbed adsorbates,[17] the persistence of the surface state feature signals that the borazine core is only weakly interacting with the substrate. Moreover, an additional broad resonance is observed at 2.3 V, reflecting an electronic feature of the BNPPy molecule, as no such signature is observed on the bare metal. Spectra taken at the coordinated pyridyl substituent (Figure 5b, green spectrum) show a pronounced resonance shifted by $\approx$350 mV toward lower energy compared to the spectral feature observed on the molecular core. Indeed, the alignment and spatial distribution of molecular orbitals can be affected by the site-specific bonding with metal adatoms as previously reported.[18,19]

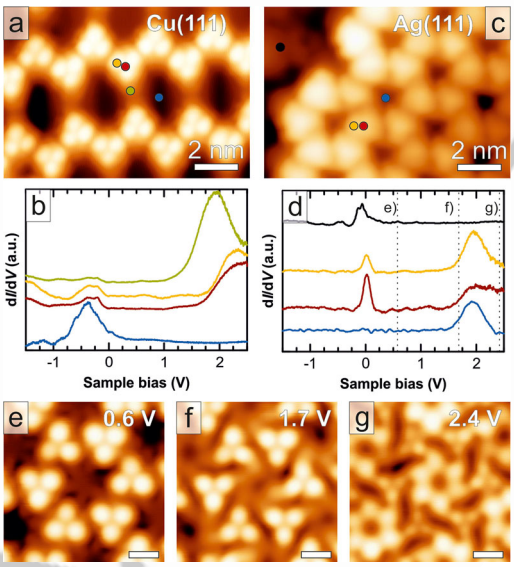

Figure 5. STM images of **BNPPy** on a) Cu(111) and c) a Ag(111) film (Scan parameters in both images: $U_b = 1.0$ V, $I_t = 100$ pA). The corresponding STS spectra recorded on characteristic positions of the respective assembly are shown in (b) and (d). e–g) Voltage series of **BNPPy** on Ag(111). (Scale bar: 1 nm. Set point: $I_t = 200$ pA).

In the case of BNPPy on the Ag(111) film, the lowest unoccupied molecular resonance is found at $\approx$2 eV and the related surface state feature at ≈ -50 meV (Figure 5d, black spectrum) is also detected on the core of the molecule (red and yellow spectrum). However, for spectra taken at the center of the pore (Figure 5c, blue dot), the surface state feature is not observed. This can be tentatively explained by the presence of the terminal pyridyl rings (see Figure 2c), which are clearly visualized in STM images only at certain bias voltage. They interact with the surface and the real pore size is drastically reduced compared to that appearing at low bias voltages. Indeed, this bias dependent contrast is revealed in an STM voltage series of BNPPy on Ag(111) displayed in Figures 5e–g. At low bias voltages, the contrast of the BNPPy molecule is dominated by the three bright protrusions in the center, while the peripheral substituents are only faintly visible (Figure 5e, $U_b = 0.6$ V). At higher bias voltages, the terminal pyridyl groups of the substituents are imaged brighter than the molecular core (Figure 5g, $U_b = 2.4$ V), indicative of unoccupied molecular resonances located on the terminal moieties.

Discussion

Using high-resolution STM imaging and X-ray diffraction, we show that individual **BNPPy** molecules have a remarkable flexibility, which is expressed by the possibility of their pyridyl-terminated substituents to bend in-plane. The terminal pyridyl groups drive the self-assembly, which can be controlled by the choice of the metal substrate. On Ag(111) and Ag(100) surfaces, the molecule-substrate interaction is weak and no influence of the surface termination on the network architecture was observed. The self-assembly is driven by intermolecular short-range vdW forces and H-bonding leading to a dense-packed network (0.34 molecules/nm^2) and no indication for metal coordination has been observed. Previous studies have been devoted to the coordination chemistry of pyridyl-functionalized molecules in the quest to achieve supramolecular networks.[20–27] In particular, utilizing Cu atoms as metallic coordination nodes, two-fold pyridyl-Cu-pyridyl coordination has been reported on Ag(111) and Cu(111).[19,20,22] However, a coordinated **BNPPy** network could not be achieved on silver surfaces, neither by annealing nor by providing additional Cu

atoms within the experimental parameter space that was explored.

Contrary to borazine derivates terminating with phenyl moieties,[13] **BNPPy** forms a highly ordered assembly on Cu(111), in which chain-like structures are formed involving Cu coordination. The resulting porous network features a packing density (0.20 molecules/nm^2) clearly reduced compared to that formed by **BNPPy** on Ag(111) and Ag(100), as well as compared to similar phenyl-terminated borazine derivatives on Cu(111) (0.33 molecules/nm^2).[13] Thus, pyridyl-mediated metal-coordination allows for the fabrication of stable borazine arrays with unprecedented pore sizes. Interestingly, this network does not reflect the three-fold symmetry of **BNPPy**, but bases on interconnected chains where only one of the three pyridyl-substituents seems to engage in Cu coordination. Even if we cannot exclude the presence of some coordinative interactions along the chains, our data suggest the simultaneous expression of metal-organic and organic bonding motifs.[28,29] The measured center-to-center distance between **BNPPy** units along the coordinated substituents—that is, perpendicular to the chain direction—is (32.2 $\pm$ 0.6) Å. With a pyridyl-substituent length of 14.4 Å, extracted from the structural model (after geometry optimization with the semi-empirical AM1 method in HyperChem[30]), this results in a projected pyridyl-Cu-pyridyl bond length of 3.4 Å, slightly reduced compared to the 3.6 Å reported in literature.[21,24,25,29] This can be rationalized by the in-plane bending of the substituents. Accordingly, the projected N–Cu bond length corresponds to 1.7 Å.

A fully reticulated coordination network with a three-fold symmetry was achieved by the deposition of additional Cu atoms. Three-fold Cu coordination has previously been reported for CN end groups,[31] bipyridyl molecules,[32] and pyridyl-terminated tectons.[21,28,33] However, for the latter case, reports on two-fold pyridyl-Cu-pyridyl coordination clearly prevail.[20–25,27,34] In the present system, the N–Cu bond distance in the three-fold node ((3.0 $\pm$ 0.5) Å) significantly exceeds the theoretically predicted value of 1.6 Å[24] and the 1.7 Å characteristic for the two-fold motif, which might reflect steric hindrance between the (nearly) co-planar pyridyl rings. Nevertheless, we cannot exclude a minor rotation of the terminal pyridyl moieties out of the surface plane. For instance, such rotations can enable a four-fold coordination of tetra-pyridyl-porphyrins to mononuclear centers.[35] We assign the coordination center to a single Cu atom (see Figure 3e), as no protrusion is apparent at the three-fold node. Protrusions were previously observed in three-fold motifs featuring Cu dimers coordinated to pyridyl termini.[21]

Our STS data on **BNPPy** and **BNAPy** molecules (Figures 5 and S32) reveal that the surface state feature is still detected on the molecular core on both the Cu(111) and the Ag substrates. This observation shows that the borazine core is decoupled from the metallic substrates by means of the dimethyl substituents, a fact which has been anticipated for similar borazine derivatives in a previous report.[13] Additionally, the binding energy of the N 1s core level is found to be 399.2 eV, comparable to the one reported for other borazine derivatives on noble metal supports,[10] and exceeding the value for *h*-BN/Cu(111) by about 1 eV.[36] The different contributions of the N atoms located in the borazine core and in the pyridyl moieties could not be resolved with our lab-based XPS setup.

Conclusion

In summary, we combined pyridyl-functionalized borazine derivatives with selected substrates to achieve distinct network architectures, exploiting the remarkable flexibility of the substituents. While the **BNPPy** molecules form a dense-packed hexagonal network on Ag substrates, a porous network evolves for **BNPPy** and **BNAPy** on Cu(111) with stability up to room temperature. The deposition of additional Cu atoms yields a structural transformation of the metal-organic architecture on Cu(111), which leads to a fully reticulated network with a three-fold pyridyl–Cu coordination motif. Following this approach, the molecular density could be varied from 0.20 to 0.18 mol nm^{-2}, expanding the corresponding pore size from 0.7 to 6.0 nm^2. These findings thus provide unprecedented metal-organic coordination architectures on surfaces based on BNC-containing molecules. Our experiments likely suggest that the presence of the sterically shielding methyl groups on the aryl B-bearing substituents prevents the adsorption of CO on the BN core, notwithstanding, they electronically decouple the BN core from the conducting substrate. This findings provide valuable insight for the design of borazine derivatives targeting the anchoring of CO in functional nanostructures comprising for example functionalized hybrid BNC polyphenylenes and graphene-like structures.[2]

Experimental Section

Most STM experiments were carried out in a custom-designed ultra-high vacuum (UHV) chamber housing a CreaTec STM operated at 5 K. Additional STM and XPS experiments were conducted at room temperature in a second UHV chamber equipped with a SPECS X-ray source with an Al anode, a SPECS PHOIBOS 100 electron analyzer and a CreaTec room temperature STM. The base pressure during all experiments was $< 5 \times 10^{-10}$ mbar. The Cu(111) and the Ag(100) single crystals were prepared by repeated cycles of Ar^+ ion sputtering and annealing to 775 and 725 K, respectively. Ag(111) films were prepared by e-beam evaporation of several layers of Ag on a Cu(111) crystal, which was held at 575 K as detailed in ref. [37]. The borazine derivatives **BNPPy** and **BNAPy** were dosed from a thoroughly degassed quartz crucible held at 600 K onto the sample held at room temperature. All STM images were recorded in constant-current mode using an electrochemically etched tungsten tip. The WSxM software was used to process the STM raw data.[38] All XP core-level spectra were excited with the Al Kα photon energy of 1486 eV. A Shirley-type background was subtracted and Voigt profiles were used to model the data.

Acknowledgements

This work is supported by the European Research Council Consolidator Grant NanoSurfs (No. 615233) and the Munich-Center for Advanced Photonics (MAP). M.G. would like to acknowledge the H2020-MSCA-IF-2014 programme. W.A. acknowledges

funding by the Deutsche Forschungsgemeinschaft via a Heisenberg professorship. D.B. thanks the Cardiff University for the financial support.

Conflict of interest

The authors declare no conflict of interest.

Keywords: borazines · coinage metals · scanning tunneling microscopy · self-assembly · surface chemistry

[1] D. Bonifazi, F. Fasano, M. M. Lorenzo-Garcia, D. Marinelli, H. Oubaha, J. Tasseroul, *Chem. Commun.* **2015**, *51*, 15222.
[2] M. M. Lorenzo-García, D. Bonifazi, *Chimia* **2017**, *71*, 550.
[3] a) I. H. T. Sham, C.-C. Kwok, C.-M. Che, N. Zhu, *Chem. Commun.* **2005**, 3547; b) P. J. Fazen, E. E. Remsen, J. S. Beck, P. J. Carroll, A. R. McGhie, L. G. Sneddon, *Chem. Mater.* **1995**, *7*, 1942.
[4] A. Wakamiya, T. Ide, S. Yamaguchi, *J. Am. Chem. Soc.* **2005**, *127*, 14859.
[5] S. Kervyn, O. Fenwick, F. Di Stasio, Y. S. Shin, J. Wouters, G. Accorsi, S. Osella, D. Beljonne, F. Cacialli, D. Bonifazi, *Chem. Eur. J.* **2013**, *19*, 7771.
[6] N. A. Riensch, A. Deniz, S. Kühl, L. Müller, A. Adams, A. Pich, H. Helten, *Polym. Chem.* **2017**, *8*, 5264.
[7] a) P. Karamanis, N. Otero, C. Pouchan, *J. Am. Chem. Soc.* **2014**, *136*, 7464; b) N. Otero, C. Pouchan, P. Karamanis, *J. Mater. Chem. C* **2017**, *5*, 8273; c) N. Otero, P. Karamanis, K. E. El-Kelany, M. Rérat, L. Maschio, B. Civalleri, B. Kirtman, *J. Phys. Chem. C* **2017**, *121*, 709.
[8] a) P. G. Campbell, A. J. V. Marwitz, S.-Y. Liu, *Angew. Chem. Int. Ed.* **2012**, *51*, 6074; *Angew. Chem.* **2012**, *124*, 6178; b) Z. Liu, T. B. Marder, *Angew. Chem. Int. Ed.* **2008**, *47*, 242; *Angew. Chem.* **2008**, *120*, 248; c) X.-Y. Wang, J.-Y. Wang, J. Pei, *Chem. Eur. J.* **2015**, *21*, 3528; d) H. Helten, *Chem. Eur. J.* **2016**, *22*, 12972.
[9] X. Wang, G. Sun, P. Routh, D.-H. Kim, W. Huang, P. Chen, *Chem. Soc. Rev.* **2014**, *43*, 7067.
[10] F. Ciccullo, A. Calzolari, I. P, S.-A. Savu, M. Krieg, H. F. Bettinger, E. Magnano, T. Chassé, M. B. Casu, *J. Phys. Chem. C* **2016**, *120*, 17645.
[11] a) K. T. Jackson, M. G. Rabbani, T. E. Reich, H. M. El-Kaderi, *Polym. Chem.* **2011**, *2*, 2775; b) T. E. Reich, S. Behera, K. T. Jackson, P. Jena, H. M. El-Kaderi, *J. Mater. Chem.* **2012**, *22*, 13524.
[12] a) F. Rosei, M. Schunack, Y. Naitoh, P. Jiang, A. Gourdon, E. Laegsgaard, I. Stensgaard, C. Joachim, F. Besenbacher, *Prog. Surf. Sci.* **2003**, *71*, 95; b) L. Piot, C. Marie, X. Feng, K. Müllen, D. Fichou, *Adv. Mater.* **2008**, *20*, 3854; c) S. Schlögl, T. Sirtl, J. Eichhorn, W. M. Heckl, M. Lackinger, *Chem. Commun.* **2011**, *47*, 12355; d) B. Cirera, J. Matarrubia, T. Kaposi, N. Giménez-Agulló, M. Paszkiewicz, F. Klappenberger, R. Otero, J. M. Gallego, P. Ballester, J. V. Barth, R. Miranda, J. R. Galán-Mascarós, W. Auwärter, D. Écija, *Phys. Chem. Chem. Phys.* **2017**, *19*, 8282.
[13] N. Kalashnyk, P. Ganesh Nagaswaran, S. Kervyn, M. Riello, B. Moreton, T. S. Jones, A. de Vita, D. Bonifazi, G. Costantini, *Chem. Eur. J.* **2014**, *20*, 11856.
[14] a) J. I. Urgel, M. Schwarz, M. Garnica, D. Stassen, D. Bonifazi, D. Écija, J. V. Barth, W. Auwärter, *J. Am. Chem. Soc.* **2015**, *137*, 2420; b) J. V. Barth, *Surf. Sci.* **2009**, *603*, 1533; c) K. Ariga, V. Malgras, Q. Ji, M. B. Zakaria, Y. Yamauchi, *Coord. Chem. Rev.* **2016**, *320 – 321*, 139; d) L. Dong, Z.'A. Gao, N. Lin, *Prog. Surf. Sci.* **2016**, *91*, 101.
[15] D. Ecija, S. Vijayaraghavan, W. Auwärter, S. Joshi, K. Seufert, C. Aurisicchio, D. Bonifazi, J. V. Barth, *ACS Nano* **2012**, *6*, 4258.
[16] C. Sánchez-Sánchez, S. Brüller, H. Sachdev, K. Mullen, M. Krieg, H. F. Bettinger, A. Nicolai, V. Meunier, L. Talirz, R. Fasel, P. Ruffieux, *ACS Nano* **2015**, *9*, 9228.
[17] J. Ziroff, P. Gold, A. Bendounan, F. Forster, F. Reinert, *Surf. Sci.* **2009**, *603*, 354.
[18] Z. Yang, M. Corso, R. Robles, C. Lotze, R. Fitzner, E. Mena-Osteritz, P. Bäuerle, K. J. Franke, J. I. Pascual, *ACS Nano* **2014**, *8*, 10715.
[19] T. R. Umbach, M. Bernien, C. F. Hermanns, L. L. Sun, H. Mohrmann, K. E. Hermann, A. Krüger, N. Krane, Z. Yang, F. Nickel, Y.-M. Chang, K. J. Franke, J. I. Pascual, W. Kuch, *Phys. Rev. B* **2014**, *89*, 235409.
[20] F. Klappenberger, A. Weber-Bargioni, W. Auwärter, M. Marschall, A. Schiffrin, J. V. Barth, *J. Chem. Phys.* **2008**, *129*, 214702.
[21] D. Heim, D. Écija, K. Seufert, W. Auwärter, C. Aurisicchio, C. Fabbro, D. Bonifazi, J. V. Barth, *J. Am. Chem. Soc.* **2010**, *132*, 6783.
[22] D. Heim, K. Seufert, W. Auwärter, C. Aurisicchio, C. Fabbro, D. Bonifazi, J. V. Barth, *Nano Lett.* **2010**, *10*, 122.
[23] A. Langner, S. L. Tait, N. Lin, R. Chandrasekar, M. Ruben, K. Kern, *Angew. Chem. Int. Ed.* **2008**, *47*, 8835; *Angew. Chem.* **2008**, *120*, 8967.
[24] Y. Li, J. Xiao, T. E. Shubina, M. Chen, Z. Shi, M. Schmid, H.-P. Steinrück, J. M. Gottfried, N. Lin, *J. Am. Chem. Soc.* **2012**, *134*, 6401.
[25] S. L. Tait, A. Langner, N. Lin, S. Stepanow, C. Rajadurai, M. Ruben, K. Kern, *J. Phys. Chem. C* **2007**, *111*, 10982.
[26] F. Studener, K. Müller, N. Marets, V. Bulach, M. W. Hosseini, M. Stohr, *J. Chem. Phys.* **2015**, *142*, 101926.
[27] T. Lin, X. S. Shang, J. Adisoejoso, P. N. Liu, N. Lin, *J. Am. Chem. Soc.* **2013**, *135*, 3576.
[28] S. Vijayaraghavan, D. Écija, W. Auwärter, S. Joshi, K. Seufert, M. Drach, D. Nieckarz, P. Szabelski, C. Aurisicchio, D. Bonifazi, J. V. Barth, *Chem. Eur. J.* **2013**, *19*, 14143.
[29] F. Bischoff, Y. He, K. Seufert, D. Stassen, D. Bonifazi, J. V. Barth, W. Auwärter, *Chem. Eur. J.* **2016**, *22*, 15298.
[30] HyperChem, Hypercube Inc., 1115 NW St., 32601, Gainesville, FL, www.hyper.com.
[31] a) G. E. Pacchioni, M. Pivetta, H. Brune, *J. Phys. Chem. C* **2015**, *119*, 25442; b) T. Sirtl, S. Schlogl, A. Rastgoo-Lahrood, J. Jelic, S. Neogi, M. Schmittel, W. M. Heckl, K. Reuter, M. Lackinger, *J. Am. Chem. Soc.* **2013**, *135*, 691; c) G. Pawin, K. L. Wong, D. Kim, D. Sun, L. Bartels, S. Hong, T. S. Rahman, R. Carp, M. Marsella, *Angew. Chem. Int. Ed.* **2008**, *47*, 8442; *Angew. Chem.* **2008**, *120*, 8570.
[32] a) A. Langner, S. L. Tait, N. Lin, R. Chandrasekar, V. Meded, K. Fink, M. Ruben, K. Kern, *Angew. Chem. Int. Ed.* **2012**, *51*, 4327; *Angew. Chem.* **2012**, *124*, 4403; b) S. L. Tait, A. Langner, N. Lin, R. Chandrasekar, O. Fuhr, M. Ruben, K. Kern, *ChemPhysChem* **2008**, *9*, 2495.
[33] L. Yan, G. Kuang, Q. Zhang, X. Shang, P. N. Liu, N. Lin, *Faraday Discuss.* **2017**, *204*, 111.
[34] a) Y. Li, N. Lin, *Phys. Rev. B* **2011**, *84*, 125418; b) Z. Shi, N. Lin, *J. Am. Chem. Soc.* **2009**, *131*, 5376.
[35] B. Wurster, D. Grumelli, D. Hötger, R. Gutzler, K. Kern, *J. Am. Chem. Soc.* **2016**, *138*, 3623.
[36] a) A. B. Preobrajenski, A. S. Vinogradov, N. Mårtensson, *Surf. Sci.* **2005**, *582*, 21; b) M. Schwarz, A. Riss, M. Garnica, J. Ducke, P. S. Deimel, D. A. Duncan, P. K. Thakur, T.-L. Lee, A. P. Seitsonen, J. V. Barth, F. Allegretti, W. Auwärter, *ACS Nano* **2017**, *11*, 9151.
[37] M. Garnica, M. Schwarz, J. Ducke, Y. He, F. Bischoff, J. V. Barth, W. Auwärter, D. Stradi, *Phys. Rev. B* **2016**, *94*, 155431.
[38] I. Horcas, R. Fernández, J. M. Gómez-Rodríguez, J. Colchero, J. Gómez-Herrero, A. M. Baro, *Rev. Sci. Instrum.* **2007**, *78*, 013705.

Manuscript received: February 21, 2018
Revised manuscript received: April 13, 2018
Accepted manuscript online: April 19, 2018
Version of record online: ■■ ■■, 0000

FULL PAPER

Surface Chemistry

M. Schwarz, M. Garnica, F. Fasano, N. Demitri, D. Bonifazi, W. Auwärter**

■■ – ■■

BN-Patterning of Metallic Substrates through Metal Coordination of Decoupled Borazines

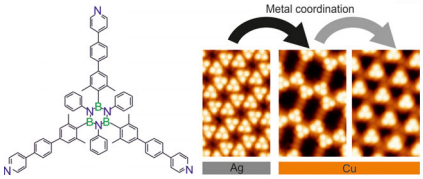

Borazine derivatives on coinage metals: Distinct network architectures are achieved by self-assembly of functionalized BNC-based tectons on Ag and Cu surfaces, featuring borazine moieties electronically decoupled from the support. On Ag, dense-packed arrays evolve. On Cu, metal-coordination steers the assembly of stable chain-like structures that transform to fully coordinated networks upon deposition of Cu atoms.

Please check that the ORCID identifiers listed below are correct. We encourage all authors to provide an ORCID identifier for each coauthor. ORCID is a registry that provides researchers with a unique digital identifier. Some funding agencies recommend or even require the inclusion of ORCID IDs in all published articles, and authors should consult their funding agency guidelines for details. Registration is easy and free; for further information, see http://orcid.org/.

Martin Schwarz
Dr. Manuela Garnica http://orcid.org/0000-0002-7861-9490
Francesco Fasano
Dr. Nicola Demitri
Prof. Dr. Davide Bonifazi
Prof. Dr. Willi Auwärter